An expanded conjugation photosensitizer with two different adsorbing groups for solar cells

Qiao-Hong Yao,[a] Lu Shan,[b] Fu-You Li,*[a] Dong-Dong Yin[b] and Chun-Hui Huang*[a]

[a] *State Key Laboratory of Rare Earth Materials Chemistry and Applications, Peking University, Beijing 100871, P. R. China. E-mail: hch@chem.pku.edu.cn; leef@chem.pku.edu.cn; Fax: +86-(10) 6275 1708; Tel: +86-(10) 6275 7156*

[b] *Department of Chemistry, Beijing Normal University, Beijing 100875, P. R. China*

Received (in New Haven, CT, USA) 6th March 2003, Accepted 15th April 2003
First published as an Advance Article on the web 7th July 2003

Three novel hemicyanine derivatives bearing different electron donors, 2-[4-*N*, *N*-dimethylaminostyryl]-*β*-naphthothiazolium propylsulfonate (dye 1), 2-[4-*N*, *N*-diethylaminostyryl]-*β*-naphthothiazolium propylsulfonate (dye 2) and 2-[2-hydroxyl-4-*N*, *N*-diethylaminostyryl]-*β*-naphthothiazolium propylsulfonate (dye 3), were designed and synthesized for use in dye-sensitized mesoporous TiO_2 solar cells. Their visible light absorption, luminescence emission, electrochemical properties, and photoelectrochemical properties were systematically studied. Upon comparison, dye 3 was found to be the best sensitizer. Experimental data show that introduction of a hydroxyl group can greatly enhance the electron injection efficiency, moreover, this enhancement can greatly override the unfavourable factor originated from the decrease of the adsorption amount of dye 3. Additionally bearing the hydroxyl group, the dye 3 sensitized solar cell gained remarkably high photoelectric conversion yield of 6.3% under illumination of 80.0 mW cm^{-2} white light from a Xe lamp.

Introduction

As an inexpensive alternative to the conventional silicon photovoltaic cell, dye-sensitized solar cell (DSSC) is attracting more and more interest because of its high photon to electron efficiencies and long life cycle.[1–3] Among the photosensitizers used in DSSC, the ruthenium polypyridyl derivatives, as a class of star dyes, have been studied extensively.[4–6] On the other hand, pure organic dyes, compared with metal complexes, have higher absorption coefficients, which could save the amount of dyes to be used and reduce the thickness of the semiconductor film. Moreover, organic dyes are easier to prepare and cost less compared with those of metal Ru based complexes. Recently, organic dye sensitized TiO_2 solar cells[7–21] have made great progress, and the highest overall yield of solar cells sensitized by pure organic dyes has exceeded 5%.[17,21] So organic dyes are promising and expected to be a new type of sensitizer for DSSCs.

In the last several years, our group has systematically studied the photoelectric conversion properties of hemicyanine dyes by the Langmuir–Blodgett technique.[22–27] Experimental results show that hemicyanine dyes with a strong donor and acceptor linked by a π-conjugation bridge can produce a higher quantum yield for photon-to-electron conversion. Later, we introduced the $-RSO_3^-$ as attaching group into hemicyanine dyes and used these dyes as photosensitizers in DSSCs. The dyes produced good charge separation properties on mesoporous TiO_2 electrode, and gave an overall light to electricity conversion of over 2%.[19,20] Recently, we found that after a pretreating of TiO_2 films with hydrochloric acid, the conversion yield of a hemicyanine dye (containing the $-RSO_3^-$ group) sensitized TiO_2 solar cell can be greatly enhanced up to 5.1%.[21] The results encouraged us to design and synthesize new hemicyanine dyes in a quest for more efficient photosensitizers.

In this paper, we describe how we designed and synthesized three new hemicyanine derivatives (Scheme 1), 2-[4-*N*, *N*-dimethylaminostyryl]-*β*-naphthothiazolium propylsulfonate (dye **1**), 2-[4-*N*, *N*-diethylaminostyryl]-*β*-naphthothiazolium propylsulfonate (dye **2**) and 2-[2-hydroxyl-4-*N*, *N*-diethylaminostyryl]-*β*-naphthothiazolium propylsulfonate (dye **3**), and systematically studied their visible light absorption, luminescence emission, electrochemical properties, and photoelectrochemical properties in order to clarify the effect of different electron donors on the photoelectric conversion properties of the dyes. Dye 3 with two adsorption functional groups was found to be the best when it served as a sensitizer and was fabricated into a solar cell.

Experimental section

Materials

Titanium(IV) tetraisopropoxide, propylene carbonate (PC), 2-methyl-*β*-nathphothiazole, 4-(dimethylamino)benzaldehyde,

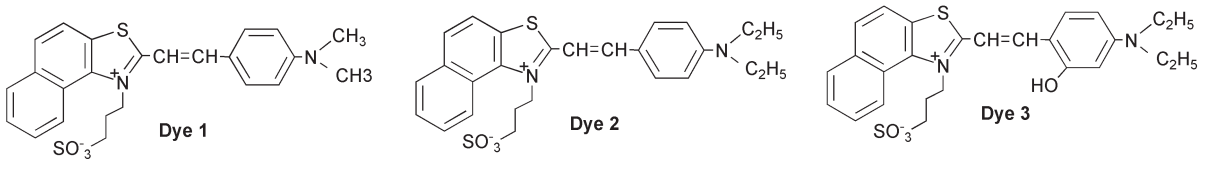

Scheme 1 Molecular structures of the three dyes.

4-(diethylamino)benzaldehyde, 4-(diethylamino)salicylaldehyde and 1,3-propane sultone were purchased from Acros. *N*-Methyl-4-methylpyridinium iodide (PyI) was synthesized according to the literature.[28] TiO_2 colloidal ethanol solution was prepared by hydrolysis of titanium(IV) tetraisopropoxide in the acidified ethanol (pH around 3) at a temperature of 0 °C.[29] All other solvents and chemicals used were produced by Beijing Chemical Factory, China (reagent grade) and used as received. Optically transparent conducting glass (CTO glass, fluorine-doped SnO_2 over layer, transmission >70% in the visible region, sheet resistance 20 Ω per square) was obtained from the Institute of Nonferrous Metals of China.

Synthesis of the photosensitizers

Dye **1** was synthesized according to the following two-step procedure,[30,31] as illustrated in Scheme 2.

Step one: synthesis of 2-methyl-β-naphthothiazolium propylsulfonate. 1.99 g (0.01 mol) 2-methyl-β-nathphothiazole and 1.22 g (0.01 mol) 1,3-propane sultone were refluxed for 48 h in 20 mL benzene. When cooled to ambient temperature, the reaction mixture was filtered and then washed with benzene to yield 2.18 g (68%) of white solid.

Step two: synthesis of dye **1**. 0.321 g (0.001 mol) 2-methyl-β-naphthothiazolium propylsulfonate and 0.149 g (0.001 mol) 4-(dimethylamino)benzaldehyde were added into 30 mL absolute ethanol and refluxed for 16 h, with piperidine as the catalyst. After being cooled to ambient temperature, the mixture was concentrated to about 10 mL and then 30 mL dimethyl ether were added. Finally, the mixture was placed in a refrigerator and kept overnight. The resulting precipitate was filtered and recrystallized from ethanol to give a purple red product: yield 78%, mp 262–263 °C. Elemental analysis: calcd for $C_{24}H_{24}N_2O_3S_2$ (%), C, 63.69; H, 5.34; N, 6.19; found, C, 63.62; H, 4.97; N, 5.92. ^{1}H NMR (500 MHz, DMSO): δ = 2.46 (m, 2H, $-CH_2SO_3^-$), 2.88 (t, 2H, $-CH_2CH_2SO_3^-$, J = 6.11 Hz), 3.12 (s, 6H, 2N–CH_3), 5.38 (t, 2H, N^+CH_2, J = 7.14 Hz), 6.84 (d, 2H, J = 8.28 Hz), 7.83 (t, 1H, CH=, J = 7.23 Hz), 7.90 (t, 1H, CH=, J = 7.82 Hz), 8.01–8.11 (m, 4H, Ar–H), 8.23–8.33 (m, 3H, Ar–H), 8.78 (d, 1H, Ar–H, J = 8.52 Hz).

Dyes **2** and **3** were synthesized according to the same procedure as dye **1** except that 4-(dimethylamino)benzaldehyde was replaced with 4-(diethylamino)benzaldehyde or 4-(diethylamino)salicylaldehyde, respectively.

Dye **2**: mp 271–272 °C. Elemental analysis: calcd for $C_{26}H_{28}N_2O_3S_2$ (%), C, 64.97; H, 5.89; N, 5.83; found, C, 64.61; H, 5.61; N, 5.61. ^{1}H NMR (500 MHz, DMSO): δ = 1.17 (t, 6H, $2NCH_2CH_3$, J = 6.60 Hz), 2.47 (m, 2H, $-CH_2SO_3^-$), 2.88 (t, 2H, $-CH_2CH_2SO_3^-$, J = 6.36 Hz), 3.51 (q, 4H, $2NCH_2$, J = 6.78 Hz), 5.36 (t, 2H, N^+CH_2, J = 7.56 Hz), 6.81 (d, 2H, Ar–H, J = 8.49 Hz), 7.82 (t, 1H, CH=, J = 7.41 Hz), 7.89 (t, 1H, Ar–H, J = 7.33 Hz), 7.96–8.07 (m, 4H, Ar–H), 8.21–8.31 (m, 3H, Ar–H), 8.77 (d, 1H, CH=, J = 8.59 Hz).

Dye **3**: mp 254–255 °C. Elemental analysis: calcd for $C_{26}H_{28}N_2O_4S_2$ (%), C, 62.88; H, 5.68; N, 5.64; found, C, 62.66; H, 5.41; N, 5.57. ^{1}H NMR (500 MHz, DMSO): δ = 1.18 (t, 6H, $2NCH_2CH_3$, J = 7.01 Hz), 2.44 (m, 2H, $-CH_2SO_3^-$), 2.86 (t, 2H, $-CH_2CH_2SO_3^-$, J = 5.80 Hz), 3.46 (q, 4H, $2NCH_2$, J = 7.09 Hz), 5.27 (t, 2H, N^+CH_2, J = 8.21 Hz), 6.21 (s, 1H, Ar–H), 6.44 (d, 1H, –CH=, J = 9.27 Hz), 7.78–7.88 (m, 3H, Ar–H), 8.10 (d, 1H, Ar–H, J = 9.09 Hz), 8.17–8.26 (m, 4H, Ar–H), 8.76 (d, 1H, –CH=, J = 8.62 Hz), 10.67 (s, 1H, –OH).

Preparation of the nanocrystalline TiO_2 electrodes

Detailed procedures for preparing nanocrystalline TiO_2 films have been described in the literature.[20,32] The thickness of TiO_2 film used in this work was *ca.* 5 μm. The TiO_2 film electrode thus obtained was coated with dye in a 3×10^{-4} mol dm^{-3} chloroform solution for at least 12 h at room temperature. After completion of the dye adsorption, the electrode was withdrawn from the solution, washed with chloroform, and dried under a stream of dry air.

Methods

^{1}H NMR spectra were recorded on a Bruker Avance 500 spectrometer, and elemental analyses were performed on a Vario EL elemental analyzer. Film thickness was determined with a DEKTAK 3 profilometer. Absorption measurements were made with a Shimadzu mode 3100UV-VIS-NIR spectrophotometer and fluorescence measurements with a Hitachi F-4500 fluorescence spectrophotometer. Cyclic voltammetry (CV) was carried out in electrochemical cells on a Model 600 voltammetric analyzer (CH Instruments, Cordova, TN). A three-electrode cell was composed of a glassy carbon as working electrode, a platinum wire as counter electrode, and a Ag/AgCl as reference electrode. The supporting electrolyte was 0.1 mol dm^{-3} $LiClO_4$ in acetonitrile. The scan rate was 0.1 V s^{-1}. All potentials reported in this work refer to the Ag/AgCl electrode.

The photovoltaic performance of the solar cells based on hemicyanine dyes was carried out in a standard two-electrode system.[3,33] Dye-coated TiO_2 film as working electrode was placed on top of an ITO glass as a counter electrode, on which the 200 nm thick Pt was sputtered. The redox electrolyte was introduced into the interelectrode space by capillary force. The solar cells were illuminated in the front through the conduction glass substrate. The effective area is 0.188 cm^2 and the redox electrolyte solution was composed of 0.5 mol dm^{-3} LiI, 0.05 mol dm^{-3} I_2, and 0.6 mol dm^{-3} *N*-Methyl-4-methylpyridinium iodide (PyI) in propylene carbonate (PC). A 500 W xenon lamp (Ushio Electric, Tokyo, Japan) served as a white light source in conjunction with an IRA-25S filter (Schott, USA) and a GG400 cutoff filter (Toshiba, Japan). Monochromatic light in the range of 400 nm to 800 nm was produced by setting an IRA-25S filter and a suitable band-pass filter (Schott, USA) in the path of the light beam before the solar cell. The incident light intensity was measured with a Light Gauge radiometer/photometer (Coherent, USA).

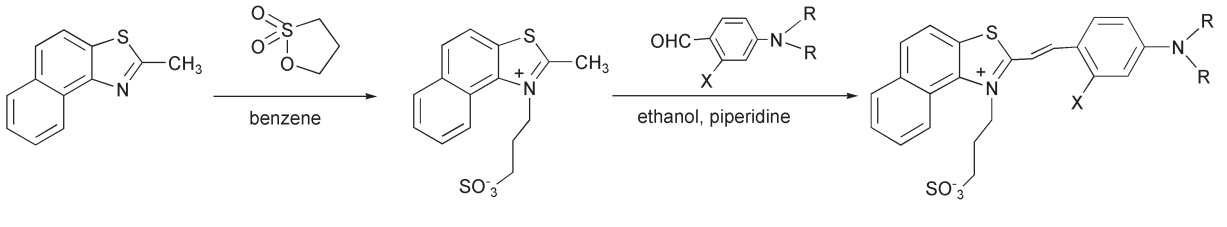

Scheme 2 The synthetic procedure of the three dyes.

Table 1 Absorption data of the hemicyanine dyes in different solvents (5×10^{-6} mol dm^{-3})

	Dye 1		Dye 2		Dye 3		
	Abs_{max} ε	(M^{-1} cm^{-1})	Abs_{max} ε	(M^{-1} cm^{-1})	Abs_{max} ε	(M^{-1} cm^{-1})	Dielectric constant
Methanol	532	13 125	542	27 667	552	43 143	32.6
Ethanol	536	5305	548	17 800	574	30 964	24.3
Pentanol	538	5556	554	18 133	566	31 125	13.9
Decanol	547	8333	557	25 350	560	32 714	8.1
Chloroform	566	6153	578	22 283	565	54 161	4.8
Acetone	531	4597	542	20 633	557	24 250	20.7
Acetonitrile	530	4431	540	26 017	554	12 214	37.5
DMSO	532	11 639	542	31 117	559	29 321	46.5
DMF	532	7333	542	21 567	565	30 089	109.5

Results and discussion

Photophysical characteristics of the dyes in solution

Absorption properties for the three dyes in different solvents are listed in Table 1, and, as an example, the absorption spectra for the three dyes in methanol are illustrated in Fig. 1. From Table 1, it is easy to find a symmetric solvatochromic effect on the photophysical behavior of dye 1 and dye 2 in linear alcohol and chloroform solvents, that is, the absorption peak of a dye in solution is normally blue shifted with increasing the polarity of solvent. In solvents other than alcohols and chloroform, the solvatochromic phenomenon became complicated due to the tendency of the molecules to form aggregates.[11,12] It is interesting to find that even in linear alcohol solvents, the maximum absorption wavelength of dye 3 did not show any solvatochromic phenomenon, indicating that the dye 3 molecules, additionally bearing a hydroxyl group, have stronger tendency to aggregate. However, an obvious tendency can be concluded from the complicated data in Table 1 that in any kind of solvents, except for acetonitrile and DMSO, the absorption maxima red shifted and the molar extinction coefficient enlarged in the sequence of dye 1, dye 2 and dye 3. We believe that this fact is originated from the increase of the delocalization extent of the dyes.

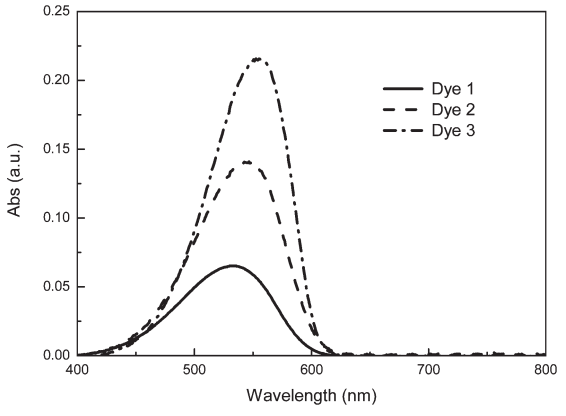

Fig. 1 Absorption spectra of the three dyes in methanol solution (5×10^{-6} mol dm^{-3}).

The luminescence properties for the three dyes in several linear alcohol solutions are also measured and the results are listed in Table 2. It appears that the fluorescence maxima red shifted slightly and the relative fluorescence intensities increased gradually for the three dyes with decreasing polarity of the solvent, that is, the relative fluorescence intensities increased when the solvents changed in the sequence methanol, ethanol, pentanol, and decanol. For example, for dye **2** in methanol solution the fluorescence maximum is at 604 nm and the relative fluorescence intensity is 4.6, while in decanol solution the former changed to 608 nm and the latter increased by a factor of 7 compared with that in methanol solution. A similar tendency was also observed for both dye **1** and dye **3**. On the other hand, in any solvent investigated (5×10^{-6} mol dm^{-3}), the change in the sequence of relative fluorescence intensity is dye **1** < dye **2** < dye **3**. For example, in ethanol solution, the relative emission intensities are 3.2, 10.4, and 36.1 for dye **1**, dye **2**, and dye **3**, respectively. The value for dye **2** is three times as high as that for dye **1**, suggesting that the replacement of the *N*,*N*-dimethyl group by an *N*,*N*-diethyl group favors fluorescence emission. Comparing dye **3** with dye **1** and dye **2**, the relative fluorescence intensity for dye **3** in ethanol solution is 11.2 and 3.5 times larger than that for dye **1** and dye **2**, indicating that, besides the replacement of the *N*,*N*-dimethyl group by an *N*,*N*-diethyl group, the introduction of hydroxyl group also favors fluorescence generation.

When TiO_2 nanoparticles are introduced into ethanol solution (10 g dm^{-3}), the relative fluorescence intensity of the three dyes is drastically decreased. The relative emission intensities decreased from 3.2, 10.4 and 36.1 to 1.4, 8.6 and 16.3 for dyes **1**, **2**, and **3**, respectively. As an example, the fluorescence spectra for dye **1** both in ethanol solution and in TiO_2 ethanol colloid solution are given in Fig. 2. Since fluorescence emission is produced by the excited electrons through deactivating from the singlet excited state to the ground state, the decreased fluorescence emission elucidated efficient electron injection from the excited state dye molecules to the TiO_2 particles.

Table 2 Fluorescence properties for the three dyes in several linear alcohol solutions (5×10^{-6} mol dm^{-3})

	Methanol		Ethanol		Pentanol		Decanol		TiO_2 colloid[a]	
	FL_{max}	$FL_{intensity}$[b]	FL_{max}	$FL_{intensity}$[b]	FL_{max}	$FL_{intensity}$[b]	FL_{max}	$FL_{intensity}$[b]	FL_{max}	$FL_{intensity}$[b]
dye **1**	602	1.7	604	3.2	606	5.3	607	6.6	603	1.4
dye **2**	604	4.6	608	10.4	608	18.3	608	33.1	608	8.6
dye **3**	600	34.3	601	36.1	603	70.4	604	132.2	600	16.3

[a] in ethanol (10 g/L). [b] arbitrary unit.

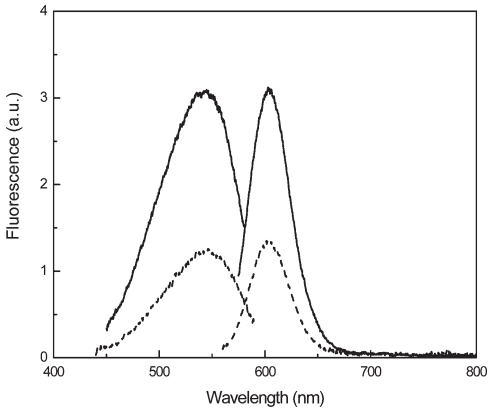

Fig. 2 Fluorescence spectra of 5×10^{-6} mol dm^{-3} dye **1** in ethanol solution (solid line) and in 10 g dm^{-3} TiO_2 ethanol colloid solution (dashed line).

Photophysical characteristics of the dyes on TiO_2 electrode

Absorption spectra of the three dyes on TiO_2 films are shown in Fig. 3. The absorption peaks for the three dyes on TiO_2 films are all extremely broadened, compared with their corresponding absorption peaks in methanol solutions (Fig. 1), suggesting that the dye molecules may aggregate in plane-to-plane stacking to form H-aggregate or in a head-to-tail arrangement to form J-aggregate,[34] when more and more dye molecules adsorb on TiO_2 film. From Fig. 3 it is easily seen that the absorption peaks of dye **1** and dye **2** are almost of the same breadth while dye **3** has a slightly narrower-band spectrum. To determine the exact amount of the dyes adsorbed on TiO_2 films, dye-coated films were soaked in methanol to desorb the dye completely. The yield solution (25 mL) was used to measure its absorbance, which was divided by the molar extinction coefficient and the thickness of liquid layer, to give the number of the dye molecules adsorbed on TiO_2 films. The number of adsorbed molecules per square centimeter TiO_2 film for the three dyes is listed in Table 3. The number for dye **1** is 2.3×10^{17}. When the *N*,*N*-dimethylanilino group is replaced by the *N*,*N*-diethylanilino group, the amount of dye **2** adsorbed decreases by about 40%. This decrease in adsorption is possibly caused by the increased steric effect. The number of adsorbed molecules for dye **3** is 4.4×10^{16}, which is about 19% of that for dye **1** and 29% of that for dye **2**. It is believed that besides the steric effect there might be other factors that cause dye **3** to have such low adsorption. Comparing the structure of dye **2**, dye **3** has a hydroxyl group on the electron donor part. This hydroxyl group can bond with the oxygen atom on the TiO_2 film through H-bonding. Considering the cooperation with other anchoring group of $-RSO_3^-$, the contact area between the dye **3** molecule and the TiO_2 nanoparticle maybe increased, which subsequently leads to a decreased adsorption of dye **3** per unit surface area of TiO_2 film. The decrease in adsorption would have a negative impact on the photoelectric conversion properties of dye **3**. Alternatively, the enlarged contact area is maybe caused by two adsorption groups existing in the molecule, which possibly favors electron injection from the excited state dye molecules to the conduction band of the TiO_2 electrode. This point of view is well supported by the data discussion later.

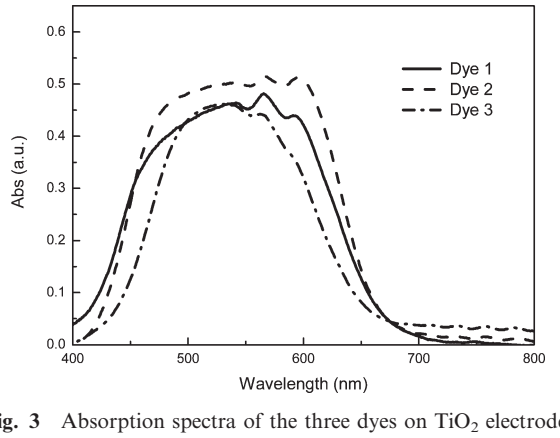

Fig. 3 Absorption spectra of the three dyes on TiO_2 electrode.

Table 3 Parameters of the dye sensitized solar cells

	I_{sc} (mA cm^{-2})	V_{oc} (mV)	*FF*	η (%)	N^a (molecules cm^{-2})	I_{sc}^b (mA molecule^{-1})
Dye **1**	10.7	496	0.616	4.1	2.3×10^{17}	4.6×10^{-17}
Dye **2**	11.1	468	0.615	4.0	1.5×10^{17}	7.4×10^{-17}
Dye **3**	15.6	512	0.631	6.3	4.4×10^{16}	3.5×10^{-16}

Illumination: 80.0 mW cm^{-2} white light from a Xe lamp. N^a: adsorption amount of dye per unit square area of TiO_2 film; I_{sc}^b: short-circuit photocurrent generated per dye molecule.

Energy levels of HOMO and LUMO

To thermodynamically judge the possibility of electron transfer from the excited dye molecules to the conduction band of TiO_2, cyclic voltammetry was performed to determine the redox potentials for the three hemicyanine dyes. Redox potentials of 0.83, 0.82 and 0.80 V *vs.* Ag/AgCl, calculated by averaging the related oxidation and reduction potentials, are roughly regarded as HOMO energy levels for dyes **1**, **2** and **3**. The absorption maximum in the visible region is at 563, 565 and 529 nm, respectively, for dyes **1**, **2** and **3**, which corresponds to the energy gap between the HOMO and LUMO energy levels for the three dyes. So the HOMO and LUMO energy levels for dye **1** are evaluated to be −5.55 eV and −3.35 eV on the absolute scale, with reference to the redox potential 0.83 V (*vs.* Ag/AgCl) and the band gap 2.20 eV (563 nm). Similarly, the HOMO and LUMO energy levels on the absolute scale are assumed to be −5.54 eV and −3.34 eV for dye **2**, −5.52 eV and −3.17 eV for dye **3**, respectively. Obviously, the excited-state energy levels for the three dyes are all higher than the energy level of TiO_2 conduction band edge (−4.40 eV),[3] showing that the electron injection should be possible thermodynamically. No emission signal was observed for the three dyes on TiO_2 films, suggesting that the injection of the excited electron from the excited dye to the TiO_2 particles is efficient.

Photoelectrochemical properties of the dye-sensitized TiO_2 electrode

Photocurrent action spectra for the dye-coated TiO_2 electrodes are shown in Fig. 4. The monochromatic incident photo-to-electron conversion efficiency (*IPCE*), defined as the number of electrons generated by light in the outer circuit divided by the number of incident photons, was obtained by the following equation:

$$IPCE(\%) = \frac{1240 I_{sc}(\mu A\,cm^{-2})}{\lambda(nm) P_{in}(W\,m^{-2})}$$

where the constant 1240 is derived from units conversion, I_{sc} is the short-circuit photocurrent generated by monochromatic light, and λ is the wavelength of incident monochromatic light, whose intensity is P_{in}. The losses of the light reflection and absorption by the conducting glass were not corrected. Comparing the action spectra with the absorption spectra on

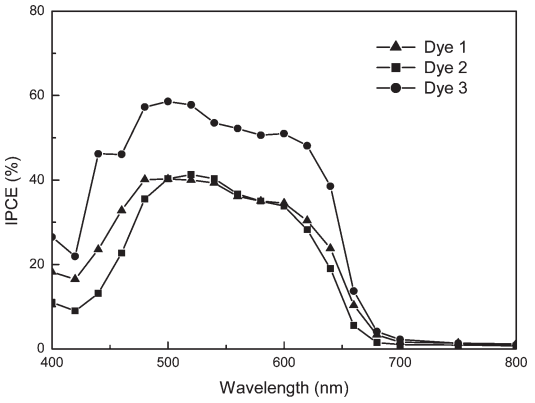

Fig. 4 Action spectra of dye sensitized TiO_2 electrodes. Effective area for illumination is 0.188 cm^{-2}; the *IPCE* values are not corrected for the loss of light intensity due to absorption by the conducting glass substrate.

TiO_2 film (*cf.* Fig. 3), all three dyes have spectral selectivity for different regions of visible light, that is, they convert more efficiently the light in the shorter wavelength region. Despite the spectral selectivity, the action spectra and the absorption spectra of the three dyes overlapped well, indicating that the photoelectrochemical conversion is achieved through photosensitization, namely that dye molecules absorbed photons and generated excited electrons and the excited electrons subsequently transferred to the conduction band of the TiO_2 electrode.[12,13] All the three dyes can efficiently convert visible light to photocurrent in the region from 400 nm to 700 nm. The maximum *IPCE* values for dyes **1** and **2** are both about 40%, while that for dye **3** is 57%. Even though the spectrum of dye **1** is a little broader than that of dye **2**, the action spectra feature of the two dyes differ little, suggesting dye that **1** and dye **2** sensitized TiO_2 electrodes would generate the same overall yield efficiency. The *IPCE* values of dye **3**, in the whole photosensitization range from 400 nm to 700 nm, are about 1.3 times higher than that of dyes **1** and **2**, therefore, dye **3** has higher electron injection efficiency than dyes **1** and **2**. From the combination of its high *IPCE* and the broad feature of its action spectrum, it is concluded that dye **3** should be a superior sensitizer to either dye **1** or dye **2**.

The photoelectrochemical properties of dye sensitized TiO_2 electrode are given in Table 3, while the photocurrent–voltage curves are shown in Fig. 5. Fill factor (*FF*) is given by the following equation:

$$FF = (V_{opt}I_{opt})/(V_{oc}I_{sc})$$

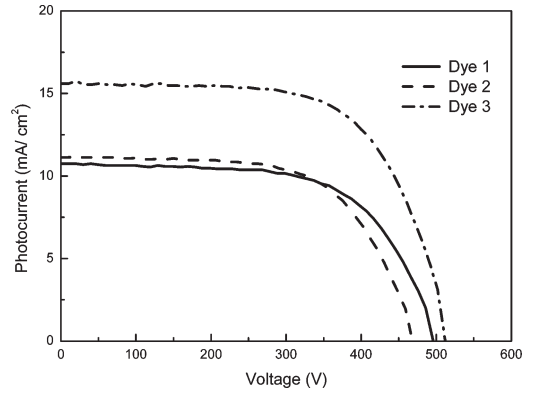

Fig. 5 Current–voltage curves of dye sensitized TiO_2 solar cells. Illumination: 80.0 mW cm^{-2} white light from a Xe lamp. Effective area: 0.188 cm^{-2}. Electrolyte: 0.5 mol dm^{-3} LiI, 0.05 mol dm^{-3} I_2 and 0.6 mol dm^{-3} PyI in PC.

where V_{opt} and I_{opt} are voltage and current for maximum power output respectively, V_{oc} and I_{sc} are open-circuit photovoltage and short-circuit photocurrent, respectively. The overall yield (η) is expressed by the following equation:

$$\eta = (V_{oc}I_{sc}FF)/P_{in}$$

where P_{in} is the power of incident white light. Here, the power of incident white light is 80.0 mW cm^{-2}. For dye **1** modified solar cell, a short-circuit photocurrent of 10.7 mA cm^{-2}, open-circuit photovoltage of 496 mV, and a fill factor of 0.616 were obtained, corresponding to an overall yield of 4.1%. According to our analysis from the action spectrum, dye **2** generated a similar value of 4.0% (with I_{sc} of 11.1 mA cm^{-2}, V_{oc} of 468 mV, and 0.615 for fill factor). Dye **3** generated the highest short-circuit photocurrent of 15.6 mA cm^{-2} due to its higher *IPCE* values in a broad range. With a higher open-circuit photovoltage of 512 mV and 0.631 for fill factor, dye **3** gained a significantly high overall yield of 6.3%.

Stability of dye 3 sensitized solar cell

In the same way as for the measurement of *I–V* curves, the stability of dye **3** on the TiO_2 electrode was tested in an unsealed solar cell under illumination of white light from a Xe lamp. Fig. 6A gives the time course of the light to electricity conversion efficiency. It was seen that the cell showed a stable efficiency up to 170 h. After that, the efficiency decreased suddenly because of an accident of the circuit. When the circuit was fixed, the efficiency recovered to the same level as before the accident, and then the efficiency decreased gradually after 200 h. From Fig. 6B, C and D, we can see that, during the time course and except for the accident, *FF* increased gradually and the V_{oc} kept almost the same, while the I_{sc} decreased slowly. Before 200 h, the efficiency remained constant because the decrease of the I_{sc} was compensated by the increase of *FF*. With the time over 200 h, *FF* increased very slowly while the I_{sc} decreased quickly. Since the two changes can not be compensated by each other, this consequently led to the decrease

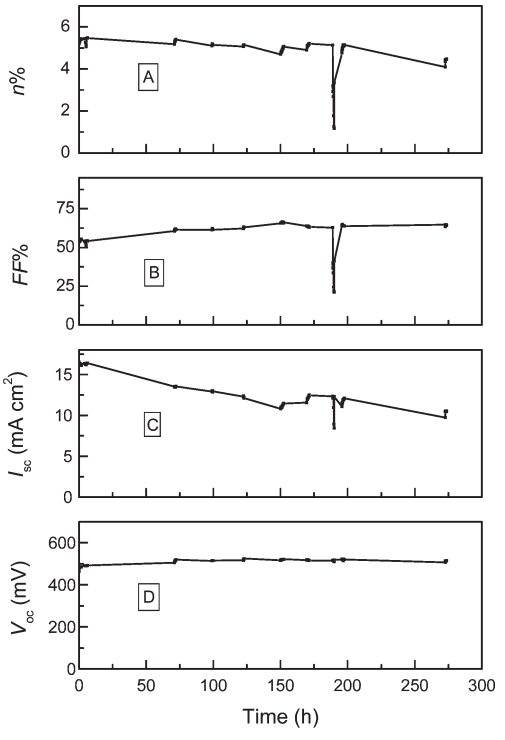

Fig. 6 Stability test of the dye **3** sensitized TiO_2 solar cell under illumination of 70.0 mW cm^{-2} white light from a Xe lamp. Other conditions as in Fig. 5.

in the efficiency. The results show that the decrease of the cell efficiency was directly due to the decrease of I_{sc}, and the main reason for the I_{sc} decrease was electrolyte loss through evaporation since the dark purple color of the dye on the electrode did not change during the stability test. Alternatively, we also checked the stability of dye **3** on TiO_2 electrode by measuring the change of the absorption properties. The dye-loaded TiO_2 film was covered with the redox electrolyte solution (50 μL cm^{-2}) to form an investigating electrode (abbr. TiO_2/D/E) after being dried in air. For comparison, the dye **3** loaded TiO_2 electrode (abbr. TiO_2/D) was also prepared and served as a reference electrode. Fig. 7 gives the time course of the maximum absorbance of the two electrodes. It was found that the absorbance of the TiO_2/D electrode decreased quickly during the first 12 hours and then decreased gradually over a prolonged time, while that of the TiO_2/D/E electrode showed almost constant during the time course (250 h). It can be concluded that the thin film of dry electrolyte can prohibit the TiO_2 film from degradation of the hemicyanine dye. This supports our belief that the main reason for the decreasing performance of the dye **3** sensitized solar cell was due to the evaporation of the solvent in the redox electrolyte solution.

Molecular structure and functional characteristic

It is well known that the *N*, *N*-diethylanilino group is a stronger electron donor than the *N*, *N*-dimethylanilino group. However the experimental data show that dye **1**, bearing the *N*,*N*-dimethylanilino group as electron donor, has a slightly higher overall photoelectric conversion yield than dye **2**. Since the short-circuit photocurrent of a dye sensitized solar cell is proportional to the amount of adsorbed dye molecules under certain conditions, so combining the value of short-circuit photocurrent and the number of adsorbed dye molecules, we can clarify the contribution of one dye molecule to the generation of the short-circuit photocurrent (ref. Table 3). Referring the number of adsorbed molecules 2.3×10^{17} molecules cm^{-2} and the short-circuit photocurrent 10.7 mA cm^{-2}, the contribution per dye **1** molecule to the short-circuit photocurrent (I_{sc}^{b}) is 4.6×10^{-17} mA. Similarly, those for dyes **2** and **3** are 7.4×10^{-17} mA and 3.5×10^{-16} mA, respectively (Table 3). Data show that the contribution of one dye **2** molecule to the short-circuit photocurrent is 60% larger than that of dye **1**, showing that replacing of the methyl group by an ethyl group is favorable for photoelectric generation. This fact agrees with the general rule. What is more interesting is the finding that the short-circuit photocurrent generated by one dye **3** molecule is 4.7 times larger than that of one dye **2**, revealing that the introduction of the additional hydroxyl group to the donor is favorable for the electron injection efficiency.

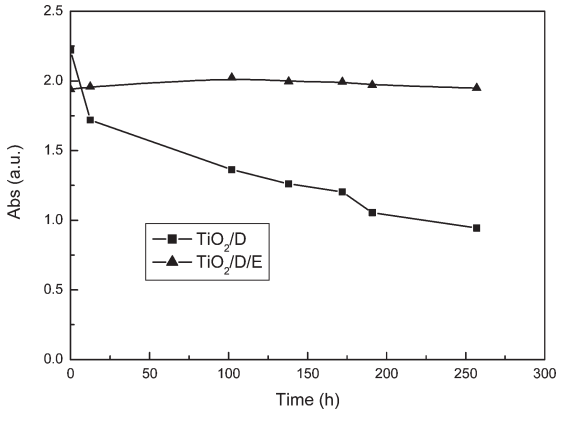

Fig. 7 Stability test of dye **3** on TiO_2 electrode.

Conclusion

Three new hemicyanine dyes, bearing the same electron acceptor but different electron donors, were synthesized and used as photosensitizer on the nanocrystalline TiO_2 electrode. Through investigation the relationship between the photoelectrochemical properties and structures of the three hemicyanine dyes, it is found that dye **3** is the best sensitizer, which has a conversion yield of 6.3%, with a short-circuit photocurrent of 15.6 mA cm^{-2}, an open-circuit voltage of 512 mV and a fill factor of 0.631 under illumination of 80.0 mW cm^{-2} white light from a Xe lamp. In addition, in an unsealed solar cell, dye **3** can generate a constant conversion yield for more than 200 h. It is found that the main reason for the gradual decrease of the efficiency after 200 h is the evaporation of the solvent in the redox electrolyte solution. Our study indicates that hemicyanine dyes could perform excellent spectral sensitization in DSSCs, and that more efficient hemicyanine dyes as sensitizers could be designed after researching the relationship between molecular structure and functional characteristic.

Acknowledgements

This work was financially supported by the State Key Program of Fundamental Research (G1998061308), and NHTRDP of P. R. China (2002 AA 324030 and 2002 AA 324080).

References

1 A. Hagfeld and M. Grätzel, *Chem. Rev.*, 1995, **95**, 49.
2 B. O'Regan and M. Grätzel, *Nature*, 1991, **353**, 737.
3 M. K. Nazeeruddin, A. Kay, I. Rodicio, R. Humphry-Baker, E. Muller, P. Liska, N. Vlachopoulos and M. Grätzel, *J. Am. Chem. Soc.*, 1993, **115**, 6382.
4 M. K. Nazeeruddin, P. Péchy and M. Grätzel, *Chem. Commun.*, 1997, 1705.
5 M. K. Nazeeruddin, P. Péchy, T. Renouard, S. M. Zakeeruddin, R. Humphry-Baker, P. Comte, P. Liska, L. Cevery, E. Costa, V. Shllover, L. Spiccia, G. B. Deacon, C. A. Bignozzi and M. Grätzel, *J. Am. Chem. Soc.*, 2001, **123**, 1613.
6 T. Renouard, R. A. Fallahpour, M. K. Nazeeruddin, R. Humphry, S. I. Gorelsky, A. B. P. Lever and M. Grätzel, *Inorg. Chem.*, 2002, **41**, 367.
7 C. Nasr, D. Liu, S. Hotchandani and P. V. Kamat, *J. Phys. Chem. B*, 1996, **100**, 11 054.
8 S. Ferrere, A. Zaban and B. A. Gregg, *J. Phys. Chem. B*, 1997, **101**, 4490.
9 N. J. Cherepy, G. P. Smestad, M. Grätzel and J. Z. Zhang, *J. Phys. Chem. B*, 1997, **101**, 9342.
10 T. N. Rao and L. Bahadur, *J. Electrochem. Soc.*, 1997, **144**, 179.
11 E. Stathatos, P. Lianos and A. Laschewsky, *Langmuir*, 1997, **13**, 259.
12 E. Stathatos and P. Lianos, *Chem. Mater.*, 2001, **13**, 3888.
13 A. Kay and M. Gratzel, *J. Phys. Chem.*, 1993, **97**, 6272.
14 A. C. Khazraji, S. Hotchandani, S. Das and P. V. Kamat, *J. Phys. Chem. B*, 1999, **103**, 4693.
15 K. Sayama, M. Sugino, H. Sugihihara, Y. Abe and H. Arakawa, *Chem. Lett.*, 1998, 753.
16 K. Sayama, K. Hara, N. Mori, M. Satsuki, S. Suga, S. Tsukagoshi, Y. Abe, H. Sugihara and H. Arakawa, *Chem. Commun.*, 2000, 1173.
17 K. Hara, K. Sayama, Y. Ohga, A. Shinpo, S. Suga and H. Arakawa, *Chem. Commun.*, 2001, 569.
18 K. Sayama, S. Tsukagoshi, K. Hara, Y. Ohga, A. Shinpou, Y. Abe, S. Suga and H. Arakawa, *J. Phys. Chem. B*, 2002, **106**, 1363.
19 Z.-S. Wang, F.-Y. Li and C.-H. Huang, *Chem. Commun.*, 2000, 2063.
20 Z.-S. Wang, F.-Y. Li, C.-H. Huang, L. Wang, M. Wei, L.-P. Jin and N.-Q. Li, *J. Phys. Chem. B*, 2000, **104**, 9676.
21 Z.-S. Wang, F.-Y. Li and C.-H. Huang, *J. Phys. Chem. B*, 2001, **105**, 9210.
22 W.-S. Xia, C.-H. Huang and D.-J. Zhou, *Langmuir*, 1997, **13**, 80.
23 T.-R. Cheng, C.-H. Huang and L.-B. Gan, *J. Mater. Chem.*, 1997, **7**, 631.

24 F.-Y. Li, J. Zheng, C.-H. Huang, L.-P. Jin, J.-Y. Zhuang, J.-Q. Guo and X.-S. Zhao, *J. Phys. Chem. B*, 2000, **104**, 5090.
25 D.-G. Wu, C.-H. Huang, L.-B. Gan, W. Zhang and J. Zheng, *J. Phys. Chem. B*, 1999, **103**, 4377.
26 D.-G. Wu, C.-H. Huang, Y.-Y. Huang, L.-B. Gan, A.-Q. Yu, L.-M. Ying and X.-S. Zhao, *J. Phys. Chem. B*, 1999, **103**, 7130.
27 C.-H. Huang, F.-Y. Li and Y.-Y. Huang, *Ultrathin Films for Optics and Electronics*, Peking University Press, Beijing, 2001, and some references therein.
28 A.-D. Lang, J. Zhai, C.-H. Huang, L.-B. Gan, Y.-L. Zhao, D.-J. Zhou and Z.-D. Chen, *J. Phys. Chem. B*, 1998, **102**, 1424.
29 Y.-X. Weng, Y. Li, Y. Liu, L. Wang, G.-Z. Yang and J.-Q. Sheng, *Chem. Phys. Lett.*, 2002, **355**, 294.
30 N. Rabjohn, R. T. Arnold and N. Leonard, *J. Org. Synth. Coll.*, 1963, **4**, 331.
31 A. Hassner, D. Birnbaum and L. M. Loew, *J. Org. Chem.*, 1984, **49**, 2546.
32 C. J. Barbé, F. Arendse, P. Comte, M. Jirousek, F. Lenzmann, V. Shklover and M. Grätzel, *J. Am. Ceram. Soc.*, 1997, **80**, 3157.
33 G. P. Smestad and M. Grätzel, *J. Chem. Educ.*, 1998, **75**, 752.
34 A. Mishra, R. K. Behera, P. K. Behera, B. K. Mishra and G. B. Behera, *Chem. Rev.*, 2000, **100**, 1973.